Chem. Res. Chinese Universities, 2019, 35(3), 463—470 doi: 10.1007/s40242-019-8369-1

A Layered Chitosan/Graphene Oxide Sponge as Reusable Adsorbent for Removal of Heavy Metal Ions

ZHANG Di, LI Ning*, CAO Shuai, LIU Xi, QIAO Mingwu, ZHANG Pingan, ZHAO Qiuyan, SONG Lianjun and HUANG Xianqing

College of Food Science and Technology, Henan Agricultural University, Zhengzhou 450002, P. R. China

Abstract Along with the growing severity of environment problem and energy crisis, it is inevitable to develop novel materials, which are contributed to the removal of hazardous pollutants from contaminated water. Herein, we reported a facile method for the preparation of free-standing chitosan/graphene oxide(CS/GO) composite sponges with low density, where CS/GO mixtures were first synthesized by the homogeneous reaction of chitosan and graphene oxide in aqueous acetic acid solution; then CS/GO sponges were obtained by lyophilizing the suspension, which were prefrozen at –20 °C and in liquid nitrogen successively. The obtained layered sponge showed good water-driven shape memory effect and was a good adsorbent of Co^{2+} and Ni^{2+} with a large adsorption capacity of 224.8 and 423.7 mg/g, respectively. Importantly, the successive adsorption-desorption studies employing CS/GO sponge indicated that the composite could be regenerated by HCl solution and reused in more than five cycles with regeneration efficiency beyond 80%. Also, the resultant sponge was explored as an exceptionally adsorbent for the removal of organic dye(*e.g.*, methylene blue, MB).

Keywords Adsorption; Heavy metal; Graphene oxide; Chitosan; Layered structure

1 Introduction

With the social process of industrialization, the problem in environmental pollution is getting worse and seriously affecting people's quality of life, which has attracted extensive attention in recent years[1,2]. Harmful contaminants in the water, such as metal ions, synthetic dyes and aromatics compounds have a serious impact on human health, especially metal ions have gained increasing attention because of their toxicity and propensity to bioaccumulate in the food chain[3]. Therefore, developing novel materials and equipment that can delivery clean and safe water to humans has continued to grab considerable attention of both scientists and engineers[4—8]. Various techniques, such as chemical precipitation, adsorption, membrane processes, biological treatment and photo catalytic degradation are employed for the removal of pollutants from wastewaters[9—11]. In particular, adsorption is the most extensively adopted method in the applications of water purification due to its low-cost, simple operation and high efficiency.

In recent years, chitosan(CS) has received considerable research interest for heavy metals removal due to its excellent metal-binding capacities and low-cost[12—16]. In addition to having biocompatible and biodegradable characteristics, the abundant amino and hydroxyl functional groups along its chemical chains endow CS with the potential ability for adsorption by forming coordination bonds with metal ions[17]. Consequently, CS exhibits a lot of promising benefits for the applications of wastewater treatment today. However, because of its inherent mechanical weakness and solubility in most dilute organic acids, it is necessary to enhance the resistance of CS against acids and chemicals through cross-linking approach.

Graphene oxide(GO), a two dimensional carbon material containing many functional groups on its basal planes and edges, has revealed great superiority as effective adsorbent for the elimination of heavy metals and organic contaminants from water due to its fascinating physical/chemical properties[18—22]. The oxygenated functional groups can act as binding sites for heavy metal ions complexation. Moreover, large available specific surface area also makes GO an outstanding candidate for water purification. It is indicated that GO could be an appropriate adsorbent for the removal of heavy metal ions, dyes and organic contaminants with high speeds and efficiencies[23—25]. In addition, GO nanosheets were reported to have the potential for cross-linking reactions with CS matrix because GO bears with oxygen-containing groups and CS possess amino groups[26]. The combination of chitosan and graphene oxide can boost its features as an adsorbent, such as binding capacity, selectivity and mechanical property, which will play an important role in enhancing the adsorption efficiency of metal ions.

Hydrogels that are hydrophilic three-dimensional(3D) polymeric networks capable of absorbing large amount of solvent have attracted great attention in the biomedical and

*Corresponding author. Email: lining8028@126.com

Received November 27, 2018; accepted February 28, 2019.

Supported by the National Natural Science Foundation of China(Nos.31201878, U1204804), the Postdoctoral Foundation of China(No.2015M572109) and the Postdoctoral Fund of Henan Province, China(No.2014049).

biotechnology fields due to their complexing abilities[27—29]. Hydrogel-based polymers functionalized with amino, carboxyl, and hydroxyl groups were reported to have potential for adsorption of pollutants from the water due to the porous structure and hydrolytic and thermal stabilities[30,31]. For example, Gao *et al*.[32] fabricated a polydopamine-functionalized graphene hydrogel, which exhibited high binding capacities toward a wide spectrum of contaminants, including heavy metals, synthetic dyes, and aromatic pollutants. Chen and coauthors[33] demonstrated that the GO-CS hydrogels could be used as absorbents to remove organic dyes(cationic MB and anionic Eosin Y) and heavy metal ions(Cu^{2+} and Pb^{2+}) from water. However, the structure of the hydrogels is relatively dense, which in turn reduced the specific surface area, leading to a low adsorption capacity. To avoid the excess stacking of the materials, aerogels and sponges with large surface area are in need of development. The 3D materials in the form of foams, aerogels and sponges possess superior properties, such as high porosity, low density and high specific surface area, for which they can be used for fabricating catalyst carriers, energy storage materials, super capacitors, and adsorbent materials[34—37].

Herein, we reporeted the preparation of CS/GO sponges by lyophilization for the removal of heavy mental ions and organic contaminants, where the CS/GO could be easily collected from the wastewater after the adsorption process. The resultant CS/GO sponge has a laminated structure and shows high adsorption capacities towards different heavy metal ions, such as Co^{2+} and Ni^{2+}. What's more, the adsorption of the hybrid could be repeated at least five times with high adsorption efficiency. The CS/GO sponge can also adsorb methylene blue(MB), which served as organic dye model, demonstrating that the CS/GO sponge has potential adsorption ability and good recyclability towards variety of metal ions and aromatic pollutions, such as Cu^{2+}, Pb^{2+}, Cd^{2+}, Hg^{2+}, benzene and its derivatives.

2 Experimental

2.1 Materials

Natural graphite powder with 325 meshes was purchased from Qingdao Huarun Graphite Co., Ltd.(Qingdao, China). Chitosan(purity ⩾ 90%, M_w=500000) was purchased from Shanghai Aladdin Reagent Co., Ltd.(Shanghai, China). All other reagents were products of Beijing Chem. Reagents Co., Ltd.(Beijing, China).

2.2 Preparation of CS/GO Sponges

Graphite oxide was prepared from graphite powder by a modified Hummer's method[38]. Chitosan was dissolved in an aqueous solution of 1%(mass fraction) acetic acid to form a 2%(mass fraction) solution. Magnetic stirring was continued for 24 h to get a viscous homogeneous liquid and then the desired amount of 5 mg/mL GO suspension was added, and the whole system was kept stirring for 12 h. The resulting CS/GO mixtures were sonicated for 30 min and then poured into Petri dish for further research. After that, the Petri dish was sealed with plastic wrap and kept at –20 °C for 10 h to allow for self-assembling into CS/GO nanocomposite hydrogel. The aerogel was then obtained after lyophilizeation for 20 h. With that, the dried free standing sponge was immersed in 1.0% NaOH solution for 1 h to neutralize the extra acetic acid, and then washed with ultrapure water to remove the residual NaOH in the composite. Finally, the CS/GO sponge was obtained by lyophilizing the above wet composite, which was prefrozen at –20 °C and in liquid nitrogen successively. The content of GO in CS/GO composite sponge was varied from 0 to 20%(mass fraction), and the pure CS sponge was prepared according to the same procedure for comparison.

2.3 Characterization

Fourier transform infrared spectra(FTIR) were obtained on a Nicolet 6700 instrument(Thermal Scientific, USA) in the range of 400—4000 cm^{-1}. Prior to the measurement, the dried samples were ground into powder and embedded in KBr disks. Scanning electron microscopy(SEM) was performed on a JSM-7401F JEOL instrument at an acceleration voltage of 15 kV.

2.4 Shape-memory Behavior Test

The pure CS and CS/15%GO sponges were selected for water-driven shape memory experiments. The sponge saturated by water was compressed to eliminate the squeezed-out solvent, and was fed with water again to recover to their original shape. The recovery rate and time were measured and compared.

2.5 Adsorption

To illustrate the adsorption capacities of CS/GO sponge, a certain amount of resultant composite was introduced into a 50-mL solution of Ni^{2+}(Co^{2+}) ions at room temperature. At defined time, the supernatant was collected and measured on a UV-Vis spectrophotometer to obtain the concentration of metal ions in the solution. The adsorption capacities of the sponges toward different adsorbates can be adjusted by changing the CS/GO mass ratio of the composites or the initial concentration of metal ions. The amount of adsorption at different time point t, q_t(mg/g), was calculated using the relationship:

$$q_t=V\times(c_0-c_t)/m \quad (1)$$

where c_0 and c_t(mg/L) denote the concentrations of metal ions at initial and defined time, respectively; V(L) is the volume of the solution; m(g) is the mass of CS/GO sponge.

The equilibrium adsorption capacity(q_e, mg/g) was defined as follows:

$$q_e=V\times(c_0-c_e)/m \quad (2)$$

where c_e(mg/L) is the concentration of metal ions at equilibrium time.

MB, served as a model organic pollutant for adsorption experiments, was chosen to investigate the adsorption capacity of the CS/GO sponges. The tests were carried out with the same methods described above. The initial concentration of the MB solution was 20 mg/L.

2.6 Adsorption-desorption

For heavy metals desorption, the sponges could be regenerated by deeply immersing in hydrochloric acid solution with a concentration of 6×10^{-3} mol/L for 45 min. Five successive cycles of adsorption-desorption using the same CS/GO composite were monitored in HCl solution to assess the regeneration and reuse ability of the sponge. Their capacities for re-adsorption of heavy metal ions(Ni^{2+} and Co^{2+}, 5 mg/mL) in repeated cycles were also monitored and compared. After each cycle of adsorption-desorption, the sponge was thoroughly washed with de-ionized water to neutrality and reconditioned for adsorption in the succeeding cycle.

3 Results and Discussion

3.1 Characterization of CS and CS/GO Sponges

The oxygenated functionalities(hydroxyl, carboxyl and carbonyl groups) of GO could be easily associated with the amino groups of CS by forming hydrogen bondings, which contributes to the facile fabrication of CS/GO composite hydrogels and sponges[26]. The self-assembly process of CS with GO nanosheets obviously resulted in a loosely packed structure of CS/GO, and the water molecules were sublimated to form sponges during the lyophilization[Fig.1(A) and (B)]. The porous CS/GO sponges were not dispersible in water, therefore could be easily separated from solution, making them convenient to collect and recyclable. On the other hand, the composites exhibit large available specific surface areas, which enable the facile applications of the resulting sponges in water purification. SEM images were obtained to illustrate the typical cross-sectional structure of pure CS and CS/GO composite sponges. It is clearly observed that the GO nanosheets are uniformly dispersed in the polymer matrix to form a layered structure after lyophilization[Fig.1(D)]. By contrast, the inside sheets of CS sponge distributed randomly, exhibiting a disordered structure as shown in Fig.1(C). The interspacing of the GO sheets wrapped with CS chain served as channel to allow the growth of the ice crystals during the freezing step(–20 °C), and the layered structure of the composite was obtained after lyophilization due to the limitation of free movement, which comes from their large specific surface area. The density of the resulting sponges with GO concentration ranged from 0 to 20%(Fig.S1, see the Electronic Supplementary Material of this paper).

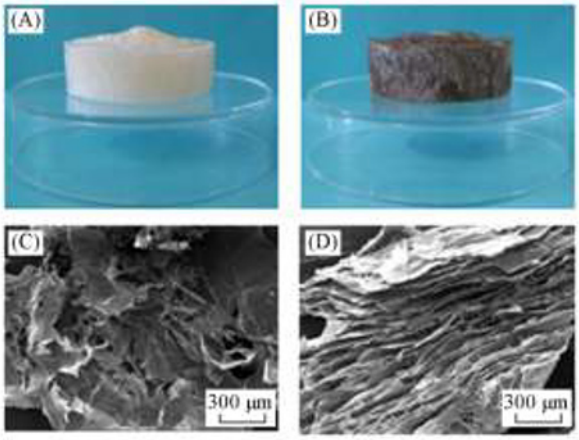

Fig.1 Appearance of the resulting CS sponge(A) and CS/GO composite sponge(B) and typical cross-sectional SEM images of CS sponge(C) and CS/GO hybrid sponge(D)

N_2 sorption measurements were carried out to investigate the pore characteristics of the CS sponge and CS/GO composite. As shown in Fig.S2(see the Electronic Supplementary Material of this paper), the surface areas of the CS and CS/GO sponges, which were calculated by the Brunauer-Emmett-Teller equation, were estimated to be 301.87 and 334.76 m^2/g, respectively. For the CS aerogel, a typical type-IV isotherm characteristic with an adsorption hysteresis indicated that there are plenty of mesopores existing in the aerogel. However, the CS/15%GO showed a type-II adsorption-desorption isotherm, corresponding to typical macroporous characteristics, which was inconsistent with their large specific surface area.

As stated in Section **1**, the functional groups of CS and GO serve as binding sites for heavy metal ions complexation. To characterize the functional groups on the components and the resulting sponges, FTIR experiments were performed as shown in Fig.2. The band due to the bending vibration of —OH and —NH_2 groups was located at around 3432 cm^{-1} in the spectrum of CS. For GO, the dominant peaks at around 3326, 2976, and 1730 cm^{-1} were ascribed to a stretching vibration from —OH or COOH, CH_3, and C═O, respectively, demonstrating the creation of oxygen-containing groups on the surface of GO nanosheets. However, the peak at 3432 cm^{-1} corresponding to the —OH and —NH_2 groups from CS sponge and CS/GO sponge shifted to an obviously lower wavenumber at 3326 cm^{-1}. Moreover, the cross linking of CS and GO was also observed by the shifting of increased adsorption band from 1730 cm^{-1} to 1722 cm^{-1}(belonging to C═O stretch of the carboxylic group), which attributed to the synergistic effect of hydrogen bonding between the two components and electrostatic interaction between polycationic CS and negatively charged GO[26].

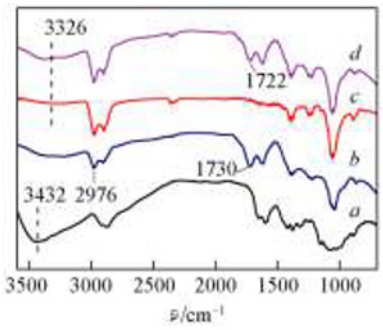

Fig.2 FTIR spectra of CS(*a*), GO(*b*), CS sponge(*c*) and CS/GO hybrid sponge(*d*)

3.2 Water-driven Shape Memory Effect

The excellent elasticity has endowed the resultant CS/GO sponges with some patent properties. Here, we found that the sponges obtained showed unique water-driven shape memory

effect. The CS/GO composite maintained the compressed shape after eliminating the squeezed-out water, and subsequently recovered its original shape within 0.5 s when fed with water again[Fig.S3(A), see the Electronic Supplementary Material of this paper]. When the sponges were compressed, plenty of new contacting points were generated and new hydrogen bondings were formed in the meantime, which helped to effectively lock the compressed deformation. Providing sufficient water again, the new formed hydrogen bondings were destroyed by the self-bonding of water molecules. Therefore, the force of fixing the compressed deformation disappeared and the materials recovered to their initial shape. Fig.S4(see the Electronic Supplementary Material of this paper) shows the typical cross-sectional SEM images of the composite sponge after squeezing and swelling. The interlayer spacing of the sample decreased when the water was squeezed out and then recovered to its initial state after swelling again, giving the conclusion that the hybrid sponge exhibited good water-driven shape memory effect. It can be seen from Fig.S3(B) that the recovery time for pure CS sponge(2 s) was longer than that of CS/GO composite under the same conditions, reflecting that the addition of GO could improve the shape memory properties of the materials. And Fig.S5(see the Electronic Supplementary Material of this paper) shows the water retention ratio of CS and CS/GO sponges as a function of cycle number.

3.3 Effect of GO Content on the Adsorption

The porous structure and excellent elasticity combined together indicated that the CS/GO sponge could be a suitable adsorbent for the extraction of organic and inorganic contaminants from the wastewater. Herein, Ni^{2+} and Co^{2+} were selected as representative heavy metal ions for evaluating the adsorption capacity of the composite sponge. The kinetics for the adsorption of Ni^{2+}(Co^{2+}) was studied in an aqueous solution with initial concentration of 5 mg/mL. To illustrate the effect of GO on the adsorption of heavy metals, five composite sponges were prepared with GO content ranging from 0 to 20%, while the mass of CS was fixed at 0.2 g. The results are shown in Fig.3. For each composite sponges containing desired amount of GO, the relatively rapid initial rates of adsorption of Ni^{2+} were seen to increase remarkably during the first 10 min and gradually reached the limiting adsorption after 120 min. Moreover, the adsorption capacity of Ni^{2+} by CS/GO sponges was strongly depended on variations of the GO concentration. It is observed from Fig.3(A) that the adsorption capacity showed a markedly increase at the range of low GO content(0—15%) and then declined with further increase in the mass fraction of GO. The additional active binding sites brought by GO were ascribed to the increase of adsorption capacity for metal ions. However, as GO content increased over 15%, the agglomeration of GO nanosheets at higher concentrations issued in a decrease in the porosity of the sponges, which in turn reduced the accessible specific surface areas, resulting in low adsorption capacity. At the same time, the kinetics for adsorption of Co^{2+} was measured as the same with those of Ni^{2+}[Fig.3(B)]. While the adsorption capacity of composite sponges showed to be higher in Ni^{2+} solution than in Co^{2+} solution under the same conditions. The varied adsorption capabilities for different metals ions may be resulted from their different complexation ability with the functional groups provided by GO and CS. It seems that Ni^{2+} tends to interact with the oxygenated groups and amino groups.

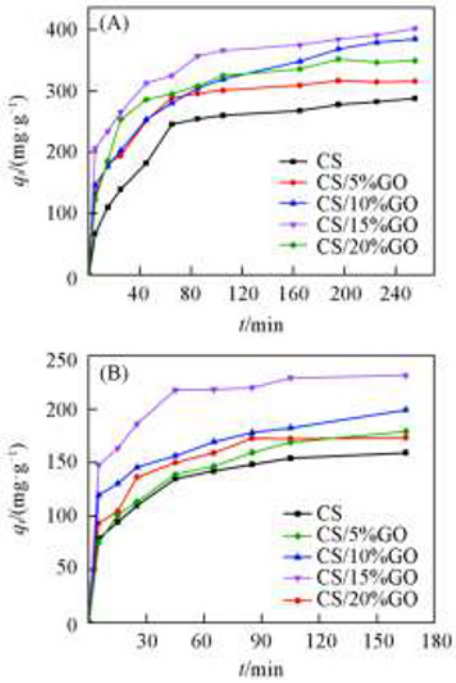

Fig.3 Effect of GO content on the adsorption of Ni^{2+}(A) and Co^{2+}(B)

Generally, the equilibrium adsorption capacity(q_e) is an important factor to determine how much adsorbent is required quantitatively for a specific solution. As can be seen in Fig.4(A), under the conditions of 5 mg of adsorbent amount,

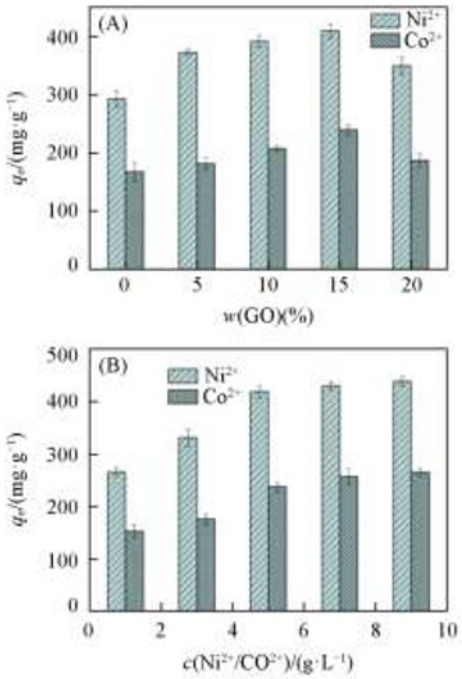

Fig.4 Effect of GO content(A) and metal ions initial concentration(B) on the equilibrium adsorption capacity of Ni^{2+} and Co^{2+}

25 °C and 5 mg/mL Ni^{2+} and Co^{2+}, the largest adsorption capacities of Ni^{2+} and Co^{2+} were 423.7 and 224.8 mg/g, respectively, on the resulting composite sponges prepared with 15% mass ratio of GO/CS.

3.4 Effect of Initial Ni^{2+}(Co^{2+}) Concentration

The adsorption isotherms of Ni^{2+} and Co^{2+} with initial concentrations in the range of 1—9 mg/mL on CS/15%GO sponges are shown in Fig.5. The binding capacity of heavy mental ions onto the composite sponge increased with an increase of contact time and gradually approached the adsorption equilibrium within 120 min for all samples. In addition, the higher the initial concentration of heavy metal ions, the larger the adsorption capacity for the CS/15% GO adsorbent. As shown in Fig.4(B), it is clear that the equilibrium adsorption capacity increased with increasing the initial Ni^{2+}(Co^{2+}) concentration in the aqueous solution. What's more, q_e increased significantly at the range of low initial concentration($\leqslant$5 mg/mL), and then the rate became slower or constant when the metal ions content was higher than 5 mg/mL. On the one hand, the higher initial amount of the heavy metal ions contributed to the increased interaction of the ions with sponges. On the other hand, the adsorption sites provided by the desired amount of adsorbent used were stationary, thus the persistent increasing of metal ions initial concentration could not increase the equilibrium adsorption capacity. The resulting maximum equilibrium adsorption capacities were 441.3 and 267.2 mg/g for Ni^{2+} and Co^{2+} with starting concentration of 9 mg/mL, respectively, under the conditions of 5 mg of adsorbent amount, 25 °C and 15% GO, which were much higher than those of CS and activated carbon adsorbents[39,40].

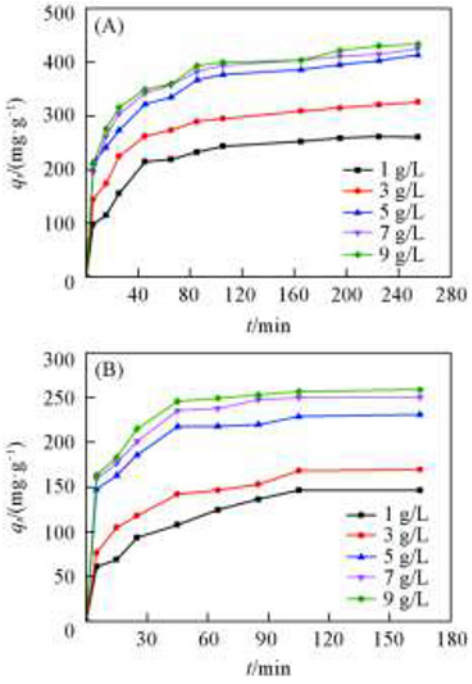

Fig.5 Effect of initial concentration on the adsorption of Ni^{2+}(A) and Co^{2+}(B)

3.5 Adsorption Isotherms

A linear fitting was applied to obtain all Langmuir and Freundlich isotherm parameters(Table S1, see the Electronic Supplementary Material of this paper). From the correlation coefficients(R) and fitting curves shown in Fig.6(A) and (C), it is obvious that the adsorption data of Ni^{2+} and Co^{2+} on CS/GO sponges were well fitted by the Langmuir model(R values are 0.992 for Ni^{2+} and 0.990 for Co^{2+}). The calculated values of the maximum adsorption capacity were 458.29 and 278.11 mg/g, respectively, close to the experimental numbers(441.3 and 267.2 mg/g). We also found that the Freundlich model fitted the data with correlation coefficients of 0.994 and 0.992 for Ni^{2+} and Co^{2+}, respectively, and the Freundlich constant n was found

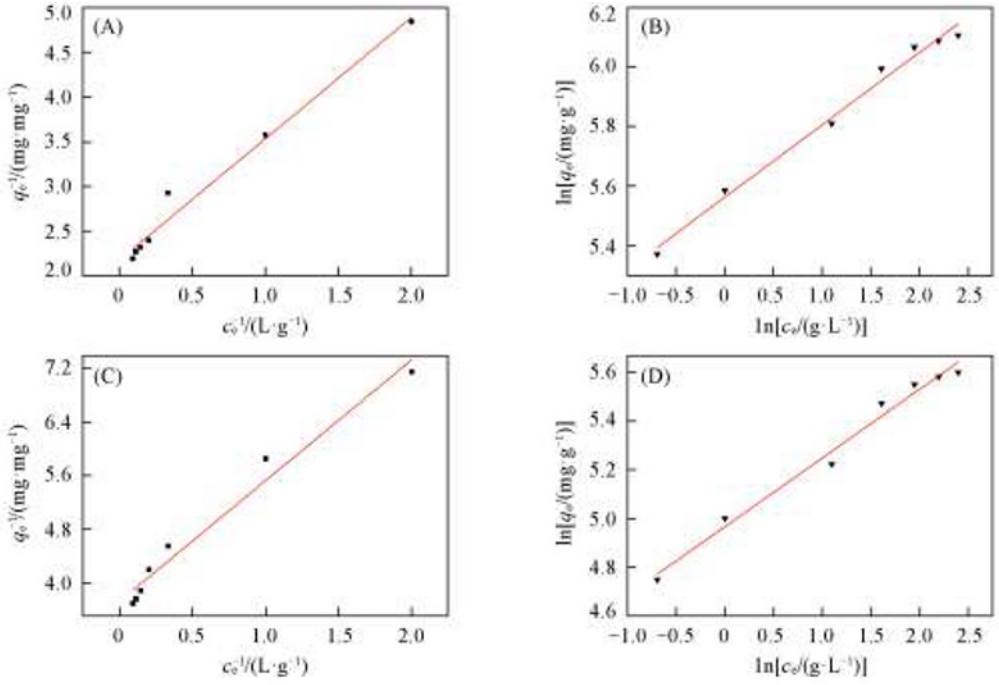

Fig.6 Adsorption of Ni^{2+}(A, B) and Co^{2+}(C, D) on CS/GO sponge

(A, C) Langmuir model; (B, D) Freundlich model.

to be greater than 1, which is a favorable condition for adsorption(4.12 for Ni^{2+}, 3.55 for Co^{2+}) as shown in Fig.6(B) and (D)[41].

3.6 Adsorption Kinetics

The kinetics of heavy metal ions removal was investigated in order to better understand the adsorption behavior of the resulting CS/GO hybrid sponge(Table S2, see the Electronic Supplementary Material of this paper). Fig.7 shows the experimental data of Ni^{2+} and Co^{2+} at different time intervals. Pseudo-first-order and pseudo-second-order models were adopted to test the kinetics data. The q_e values calculated from the pseudo-first-order model were 212.65 and 98.14 mg/g, much lower than the experimental values for Ni^{2+} and Co^{2+}, respectively(423.7 and 224.8 mg/g). Moreover, small correlation coefficients were found in the straight-line plot in Fig.7(A) and (C)(0.956 for Ni^{2+}, 0.930 for Co^{2+}). The fact suggested that the pseudo-first-order model was not suitable for describing the adsorption behavior of Ni^{2+} and Co^{2+} on CS/GO composites. In contrast, the kinetic data for the adsorbent were property fitted to the pseudo-second-order model as shown in Fig.7(B) and (D)(R values were 0.9995 for Ni^{2+}, 0.9991 for Co^{2+}). The calculated values of adsorption capacity for Ni^{2+} and Co^{2+}(429.84 and 232.21 mg/g) were close to those of experimental adsorption capacity. The results indicated that heavy metal ions contraction onto CS/GO sponges is favorable by the pseudo-second-order model[12].

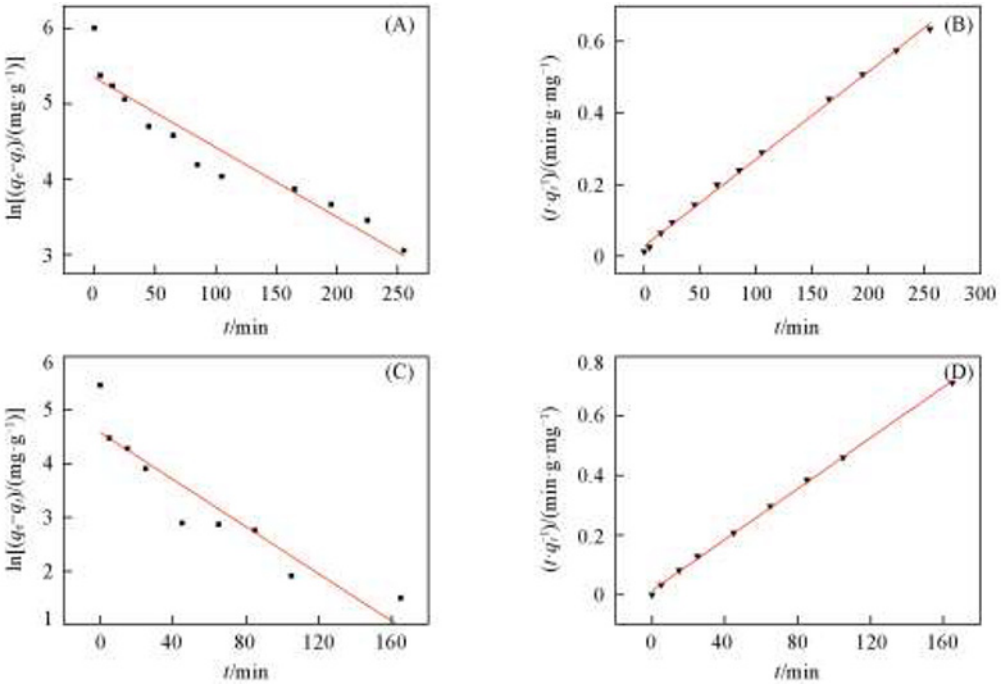

Fig.7 Kinetics analyses of the adsorption of Ni^{2+}(A, B) and Co^{2+}(C, D) on CS/GO sponge

(A, C) Pseudo-first-order model; (B, D) pseudo-second-order model.

3.7 Filtration-adsorption of the Metal Ions

The above adsorption experiments were carried out in the absence of any mechanical agitations, therefore, the random molecular motions, metal ions diffusion are the dominant driving force for adsorption process. The solid sponges could be shaken in pollutant solution to accelerate the adsorption rate, which was widely used for graphene sponge, aerogel and hydrogel[24,42]. In this study, 0.27 g of sponges of CS with 15% GO was made into a cylindrical shape and placed in the tube of a column as shown in the insets of Fig.8(A) and (B). Then, 15 mL of sewage with an initial Ni^{2+}(Co^{2+}) concentration of 5 mg/mL passed through the pores of CS/GO sponge, where the contaminants were adsorbed by the adsorbent to achieve the

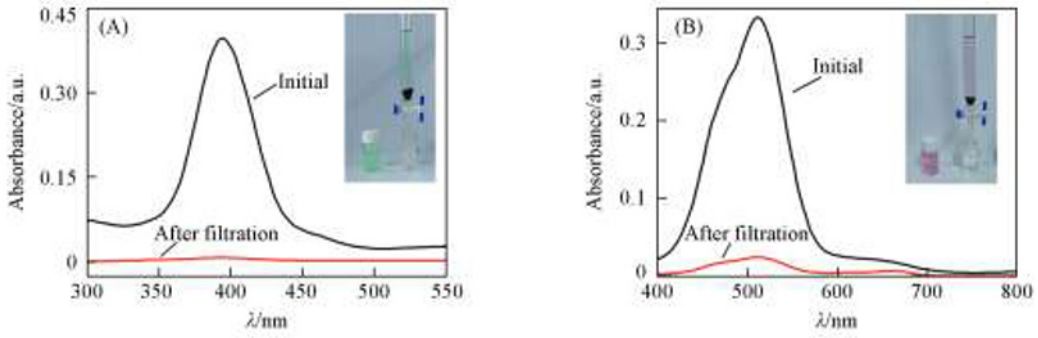

Fig.8 Absorbance spectra of Ni^{2+}(A) and Co^{2+}(B) before and after filtration

Insets of (A) and (C): photographs of adsorption columns using CS/GO sponge for separating Ni^{2+} and Co^{2+} from water, respectively.

purpose of water purification. After 30 min adsorption, the colorful heavy metal ions solution changed into colorless and the sponges could be used for many times. In addition, the ultraviolet adsorption spectra of Ni^{2+} and Co^{2+} before and after filtration have been studied and the results are shown in Fig.8(A) and (B). The metal ions were basically removed by CS/GO composite after 30 min, reflecting a high speed and efficiency of sewage treatment.

3.8 MB Adsorption

MB was selected as a model organic pollutant to access the ability of the CS/GO composite for adsorptive removal of organic contaminants from water. The resulting sponge of CS/15%GO(5 mg) was added to 25 mL of 20 mg/L MB solutions without stirring. At pre-set time intervals, the sample was removed from the solution by decantation. Fig.9 shows the time profile of MB adsorption on the CS/GO composite sponges. The absorbance of MB significantly decreased as the time grows, indicating that the sponge can be used for the removal of organic pollutant. The solution containing 1 mg/L MB changed into colorless after 72 h as is shown in Fig.S6(A)(see the Electronic Supplementary Material of this paper). However, the efficiency is rather low for static adsorption on the resulting sponges. The maximum adsorption capacity of MB solution with initial concentration of 20 mg/L was 14.8 mg/g under the conditions of 5 mg of adsorbent amount, 25 °C and 15% GO [Fig.S6(B)]. Compared to pure CS, GO was found to be capable of interacting with a MB molecule through π-π conjugation and electrostatic interaction, thus could facilitate the adsorption capacity of the as-prepared hybrid sponge. To achieve the adsorption process with high speed and efficiency, the adsorbent was produced in the form of cylinder for the removal of dye molecules(4 mg/L) from water by filtering(the inset of Fig.10). The ultraviolet adsorption spectrum of MB before and after filtration is shown in Fig.10. The absorbance of MB after CS/GO sponge treatment decreased significantly, giving the conclusion that the resultant composites have good interception efficiency for MB molecules.

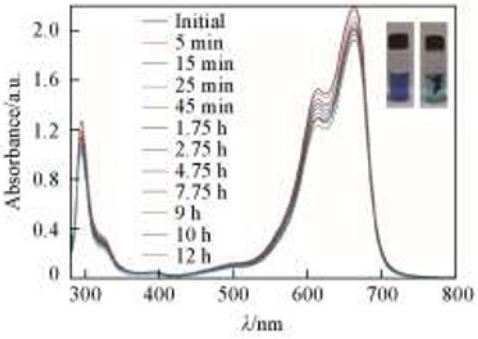

Fig.9 Time-dependent absorbance of MB solution(20 mg/L)

The insets show the dye solutions before and after the addition of the CS/GO sponge, respectively.

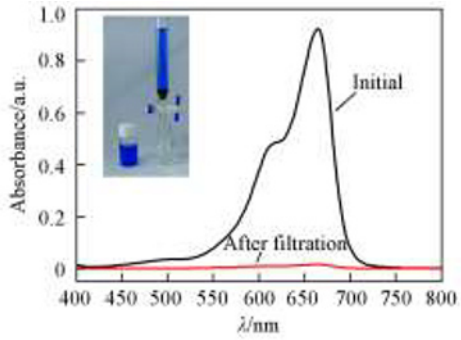

Fig.10 Absorbance spectra of MB solution(4 mg/L) before and after filtration using GS/GO sponge

The inset shows the photograph of MB removal from water by filtration using CS/GO sponge.

3.9 Reusability for Metal Ions Removal

The adsorption-desorption experiments were performed to evaluate the regeneration and reuse ability of the resultant adsorbents for practical applications. HCl solution(6×10^{-3} mol/L) was chosen as the desorption agent to recover Ni^{2+} and Co^{2+} from the absorbed CS/GO sponges. Fig.11(A) shows the effect of recycling times on the equilibrium adsorption capacity of heavy metal ions. The adsorption capacities decrease for each pollutant after five cycles because of the structure breakage due to the acid treatment during the desorption process. While the values of regenerated sponges are still much high, and beyond 80% of its maximum adsorption capacities were retained for these metal ions after 5 cycles(83.57% for Ni^{2+}, 84.10% for Co^{2+}) as shown in Fig.11(B). And Fig.S7(see the Electronic Supplementary Material of this paper) shows the adsorption capacities for Cu^{2+}, Pb^{2+}, Cd^{2+} and Hg^{2+}(81.36% for Cu^{2+}, 80.67% for Pb^{2+}, 82.78% for Cd^{2+} and 83.05% for Hg^{2+}). In contrast, the partial collapse of its networks in acidic solution makes pure CS sponge unable to reuse for multiple times. The excellent adsorption capacities and good recyclability suggest

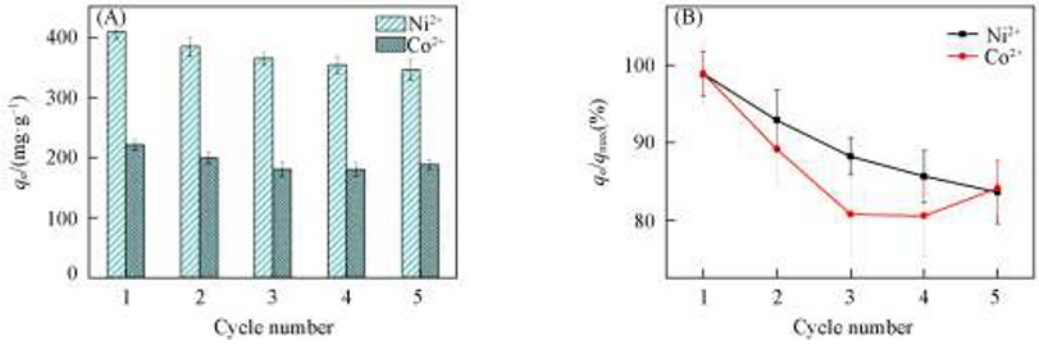

Fig.11 Regenerated equilibrium adsorption capacity of CS/GO sponge(A) and adsorption efficiency of CS/GO sponge with respect to recycling times(B)

that the CS/GO composite sponges can be used as an ideal adsorbent for the removal of heavy metal ions.

It is strongly obvious that CS/GO sponges are ideal candidates as high-capacity adsorbents for the adsorption of heavy metal ions and organic contaminants, which concurs with the results described in the other CS-based aerogels[8,20,37]. Moreover, the CS/GO composite sponges obtained by lyophilization have layered structures, which provides a new route for the fabrication of biomimetic materials.

4 Conclusions

In conclusion, the layered CS/GO composite sponges with commendable performance of efficient adsorption have been successfully fabricated by self-assembly of CS with GO nanosheets under acidic conditions followed by lyophilization. The flexible and tough sponge exhibited unique water-driven shape memory properties, and was also found to be an ideal candidate as high-capacity adsorbent towards heavy metal ions and organic contaminants. Furthermore, the resulting composite could be easily separated from aqueous solution by decantation, regenerated and reused in more than five cycles of adsorption-desorption, showing a good recyclability. These findings indicate that the CS/GO composite sponges show huge potential in heavy mental ions and organic pollutants adsorptions.

Electronic Supplementary Material

Supplementary material is available in the online version of this article at http://dx.doi.org/10.1007/s40242-019-8369-1.

References

[1] Blanchard G., Maunaye M., Martin G., *Water Res*., **1984**, *18*, 1501

[2] Lei Y. L., Chen F., Luo Y. J., Zhang L., *Chem. Phys. Lett.*, **2014**, *593*, 122

[3] Li Q., Zhao Y., Qu D., Wang H., Chen J., Zhou R., *Chem. Res. Chinese Universities*, **2018**, *34*(5), 808

[4] Yi J. C., Mei F. C., Law C. L., Hassell D. G., *Chem. Eng. J.*, **2009**, *155*, 1

[5] Yan H., Yang L. Y., Yang Z., Yang H., Li A. M., Cheng R. S., *J. Hazard. Mater.*, **2012**, *229*, 371

[6] Jiang T. S. , Liu W. P., Mao Y. L., Zhang L., Cheng J. L., Gong M., Zhao H. B., Dai L. M., Zhang S., Zhao Q., *Chem. Eng. J.*, **2015**, *259*, 603

[7] Du R., Zhang N., Xu H., Mao N. N., Duan W. J., Wang J. Y., Zhao Q. C., Liu Z. F., Zhang J., *Adv. Mater.*, **2014**, *26*, 8053

[8] Wan Ngah W. S., Teong L. C., Hanafiah M. A. K. M., *Carbohydr. Polym.*, **2011**, *83*, 1446

[9] Ghaee A., Shariaty-Niassar M., Barzin J., Zarghan A., *Appl. Surf. Sci.*, **2012**, *258*, 7732

[10] Hu Z., Lei L., Li Y., Ni Y., *Sep. Purif. Technol*., **2003**, *31*, 13

[11] Reddad Z., Gerente C., Andres Y., Thibault J. F., Le Cloirec P., *Water Res.*, **2003**, *37*, 3983

[12] Wang G. H., Liu J. S., Wang X. G., Xie Z. Y., Deng N. S., *J. Hazard. Mater.*, **2009**, *168*, 1053

[13] Yang F., Liu H. J., Qu J. H., Paul Chen J., *Bioresour. Technol.*, **2011**, *102*, 2821

[14] Liu D. G., Li Z. H., Zhu Y., Li Z. X., Kumar R., *Carbohydr. Polym.*, **2014**, *111*, 469

[15] Eser A., Tirtom V. N., Aydemir T., Becerik S., Dinçer A., *Chem. Eng. J.*, **2012**, *210*, 590

[16] Petrova Y. S., Pestov A. V., Usoltseva M. K., Neudachina L. K., *J. Hazard. Mater.*, **2015**, *299*, 696

[17] Babel S., Kurniawan T. A., *J. Hazard. Mater.*, **2003**, *B97*, 219

[18] Vilela D., Parmar J., Zeng Y., Zhao Y., Sánchez S., *Nano Lett.*, **2016**, *16*, 2860

[19] Peng W. J., Li H. Q., Liu Y. Y., Song S. X., *J. Mol. Liq.*, **2017**, *230*, 496

[20] Li Y. H., Du Q. J., Liu T. H., Sun J. K., Wang Y.H., Wu S. L., Wang Z. H., Xia Y. Z., Xia L. H., *Carbohydr. Polym.*, **2013**, *95*, 501

[21] Yu J. G., Yu L. Y., Yang H., Liu Q., Chen X. H., Jiang X. Y., Chen X. Q., Jiao F. P., *Sci. Total Environ.*, **2015**, *502*, 70

[22] Zhang Y., Zhang S., Gao J., Chung T. S., *J. Membr. Sci.*, **2016**, *515*, 230

[23] Liu Q., Shi J. B., Sun J. T., Wang T., Zeng L. X., Jiang G. B., *Angew. Chem. Int. Ed.*, **2011**, *123*, 6035

[24] Lin Y., Xu S., Li J., *Chem. Eng. J*., **2013**, *225*, 679

[25] Zhao G., Jiang L., He Y., Li J., Dong H., Wang X., Hu W., *Adv. Mater.*, **2011**, *23*, 3959

[26] Zhang Y. Q., Zhang M., Jiang H. Y., Shi J. L., Li F. B., Xia Y. H., Zhang G. Z., Li H. J., *Carbohydr. Polym.*, **2017**, *177*, 116

[27] Trakulsujaritchok T., Noiphom N., Tangtreamjitmun N., Saeeng R., *J. Mater. Sci.*, **2011**, *46*, 5350

[28] Kasgoz H., Ozgumus S., Orbay M., *Polymer*., **2003**, *44*, 1785

[29] Milosavljević N. B., Milašinović N. Z., Popović I. G., Filipović J. M., KalagasidisKrušić M. T., *Polym. Int.*, **2011**, *60*, 443

[30] Akkaya R., Ulusoy U., *J. Hazard. Mater.*, **2008**, *151*, 380

[31] Wang M., Xu L., Peng J., Zhai M. L., Li J. Q., Wei G. S., *J. Hazard. Mater.*, **2009**, *171*, 820

[32] Gao H. C., Sun Y. M., Zhou J. J., Xu R., Duan H. W., *ACS Appl. Mater. Interfaces.*, **2013**, *5*, 425

[33] Chen Y. Q., Chen L. B., Bai H., Li L., *J. Mater. Chem. A*, **2013**, *1*, 1992

[34] Long Y., Zhang C. C., Wang X. X., Gao J. P., Wang W., Liu Y., *J. Mater. Chem.,* **2011**, *21*, 13934

[35] Shin Y. J., Wang Y. Y., Huang H., Kalon G., Wee A. T. S., Shen Z. X., Bhatia C. S., Yang H., *Langmuir*, **2010**, *26*, 3798

[36] Chen M., Tao T., Zhang L., Gao W., Li C., *Chem. Commun.*, **2013**, *49*, 1612

[37] Zhao J. W., Ren W., Cheng H. M., *J. Mater. Chem.*, **2012**, *22*, 20197

[38] Zhang Y. Q., Jiang H. Y., Li F. B., Xia Y. H., Lei Y., Jin X. H., Zhang G. Z., Li H. J., *J. Mater. Chem. A*, **2017**, *5*, 14604

[39] Ghaee A., Shariaty-Niassar M., Barzin J., Zarghan A., *Appl. Surf. Sci*., **2012**, *258*, 7732

[40] Corapcioglu M. O., Huang C. P., *Water Res*., **1987**, *21*, 1031

[41] Yu B. W., Xu J., Liu J. H., Yang S. T., Luo J. B., Zhou Q. H., Wan J., Liao R., Wang H. F., Liu Y. F., *J. Environ. Chem. Eng.*, **2013**, *1*, 1044

[42] Liu F., Chung S., Oh G., Seo T. S., *ACS Appl. Mater. Interfaces*, **2012**, *4*, 922